Molecular Cancer Therapeutics

Selective Killing of SMARCA2- and SMARCA4-deficient Small Cell Carcinoma of the Ovary, Hypercalcemic Type Cells by Inhibition of EZH2: *In Vitro* and *In Vivo* Preclinical Models

Elayne Chan-Penebre, Kelli Armstrong, Allison Drew, Alexandra R. Grassian, Igor Feldman, Sarah K. Knutson, Kristy Kuplast-Barr, Maria Roche, John Campbell, Peter Ho, Robert A. Copeland, Richard Chesworth, Jesse J. Smith, Heike Keilhack, and Scott A. Ribich

Abstract

The SWI/SNF complex is a major regulator of gene expression and is increasingly thought to play an important role in human cancer, as evidenced by the high frequency of subunit mutations across virtually all cancer types. We previously reported that in preclinical models, malignant rhabdoid tumors, which are deficient in the SWI/SNF core component INI1 (SMARCB1), are selectively killed by inhibitors of the H3K27 histone methyltransferase EZH2. Given the demonstrated antagonistic activities of the SWI/SNF complex and the EZH2-containing PRC2 complex, we investigated whether additional cancers with SWI/SNF mutations are sensitive to selective EZH2 inhibition. It has been recently reported that ovarian cancers with dual loss of the redundant SWI/SNF components SMARCA4 and SMARCA2 are characteristic of a rare rhabdoid-like subtype known as small-cell carcinoma of the ovary hypercalcemic type (SCCOHT). Here, we provide evidence that a subset of commonly used ovarian carcinoma cell lines were misdiagnosed and instead were derived from a SCCOHT tumor. We also demonstrate that tazemetostat, a potent and selective EZH2 inhibitor currently in phase II clinical trials, induces potent antiproliferative and antitumor effects in SCCOHT cell lines and xenografts deficient in both SMARCA2 and SMARCA4. These results exemplify an additional class of rhabdoid-like tumors that are dependent on EZH2 activity for survival. *Mol Cancer Ther; 16(5); 850–60. ©2017 AACR.*

Introduction

EZH2, an enzymatic subunit of the polycomb-repressive complex 2 (PRC2,) catalyzes the methylation of H3K27, thereby repressing target gene transcription. EZH2 is amplified, overexpressed, or mutated in multiple cancer types, most notably follicular lymphoma (FL) and germinal center diffuse large B-cell Lymphoma (DLBCL). We and others have shown that pharmacologic inhibition of EZH2 can block proliferation and survival in a subset of cancer cell lines, supporting its function as an oncogene (1–7). In addition to posttranslational modifications of chromatin, gene transcription is also regulated by the ATP-dependent remodeling of chromatin structure. The SWItch/Sucrose Non-Fermentable (SWI/SNF) complex is a chromatin-remodeling complex that alters the position of nucleosomes along DNA, thus relieving steric barriers that make gene promoter regions more accessible to transcription factors and key cellular proteins (8). Two SWI/SNF complexes exist in humans: the BAF (BRG1-associated factors) and PBAF (Polybromo-associated BAF) complexes each consisting of combinatorial assemblies of approximately 15 subunits. It is now well established that SWI/SNF subunits are frequently mutated in many tumor types, and have been clearly shown to have a tumor suppressor function (8–10).

One such subunit, SMARCB1 (INI1, SNF5, or BAF47), a core component of the SWI/SNF complex, is inactivated via biallelic mutations in virtually all malignant rhabdoid tumors (MRT) and atypical teratoid rhabdoid tumors (ATRT; refs. 11, 12). MRTs and ATRTs are highly aggressive cancers with poor prognosis and no effective chemotherapies that mainly affect children. We and others have previously reported an antagonistic relationship between EZH2 and SMARCB1 such that SMARCB1-deficient cancers are dependent on EZH2 oncogenic activity (3, 13). We have demonstrated that cell lines and xenografts deficient in SMARCB1 are sensitive to the selective EZH2 inhibitor tazemetostat (EPZ006438; ref. 3), resulting in potent antiproliferative effects *in vitro* and durable tumor regressions *in vivo*. These preclinical data support the hypothesis that rhabdoid tumors are dependent on PRC2 activity, which is dysregulated in SMARCB1-deficient tumors; this leads to the aberrant repression of polycomb target genes, such as those involved in differentiation and tumor suppression. Similarly, we and others have recently shown that mutation of another SWI/SNF member, SS18, in synovial sarcoma, also results in a dependence on EZH2 activity (4, 14, 15).

In addition to the mutations in SMARCB1 and SS18 described above, there are an increasing number of reports describing

Epizyme Inc., Cambridge, Massachusetts.

Note: Supplementary data for this article are available at Molecular Cancer Therapeutics Online (http://mct.aacrjournals.org/).

E. Chan-Penebre and K. Armstrong contributed equally to this article.

Corresponding Author: Scott A. Ribich, Epizyme Inc., 400 Technology Square, Cambridge, MA 02139. Phone: 617-500-0615; Fax: 617-349-0707; E-mail: sribich@epizyme.com

doi: 10.1158/1535-7163.MCT-16-0678

deleterious mutations in other SWI/SNF complex members across many different human cancers (8–10). SMARCA4 and SMARCA2 are the two mutually exclusive ATPase catalytic subunits of the SWI/SNF complex that have postulated tumor suppressor roles in cancers such as non–small cell lung cancer (NSCLC; refs. 16, 17). In addition, multiple reports indicate that the expression of SMARCA4 and SMARCA2 are concomitantly lost in a subset of NSCLC (16–18). Interestingly, in a rare type of ovarian cancer, small-cell carcinoma of the ovary, hypercalcemic type (SCCOHT), *SMARCA4* and *SMARCA*2 have been found to be coinactivated. SMARCA4 activity is lost via genomic mutations, whereas SMARCA2 mRNA is lost in the absence of any coding mutations (19–24). Increasing evidence now suggests that the dual loss of SMARCA2 and SMARCA4 is a molecular signature and defining feature of SCCOHT. Reexpression of either ATPase in SCCOHT cell lines have been shown to inhibit cell growth emphasizing the importance of SMARCA2 and SMARCA4 dual loss in SCCOHT (24).

SCCOHT is a rare and lethal subtype of ovarian cancer that mainly affects adolescent and young adult women (25, 26). Most SCCOHT patients receive a combination of surgery and multiagent chemotherapy, but the large majority either do not respond or rapidly relapse following treatment with available therapies; hence, the one-year overall survival rate for SCCOHT patients is only 50%. Interestingly, SCCOHT tumors share many similarities with rhabdoid tumors (20, 21, 27, 28). They are both aggressive forms of cancer that respond poorly to conventional therapy. Histologically, both tumors consist of sheet-like arrangements of small, tightly packed, highly proliferative, and undifferentiated cells. In addition, the genomes of both SCCOHT and rhabdoid tumors, are mutationally quiet with few if any mutations other than genetic alterations of the SWI/SNF complex (19, 20, 22). Given the clinical, pathologic, and molecular similarities between SCCOHT and rhabdoid tumors, we sought to investigate the effects of EZH2 inhibition in SMARCA2- and SMARCA4-deficient (SCCOHT) ovarian cancers.

Using the criteria that dual SMARCA2- and SMARCA4 deficiency define SCCOHT cell lines, we identified three previously misclassified SCCOHT cell lines. We find that EZH2 inhibition, using our highly selective and potent inhibitor tazemetostat, led to robust antiproliferative effects in ovarian cell lines that lacked both SMARCA2 and SMARCA4. Furthermore, we observed potent antitumor effects in SCCOHT cell line xenograft models treated with tazemetostat.

Materials and Methods

Tissue culture and cell lines

Cell lines used in these experiments were obtained from the following sources between 2012 and 2016. Cell lines were cultured according to conditions specified by the respective cell banks. From ATCC: TOV112D (CRL-11731), COAV-3, OCVAR-3 (HTB-161), OV90 (CRL-11732), SK-OV-3 (HTB-77), and PA-1 (CRL1572). From DSMZ: EFO-27 (AAC 191). From SIBS: HO8910 (TCHu 24). From JCRB: TYK-NU (JCRB023.0), KURAMOCHI (JCRB00098), RKN (JCRB0176), RMUG-S (IFO50320), OVSAHO (JCRB1046), OVTOKO (JCRB1048), OVISE (JCRB1043), OVMANA (JCRB1045), RMG-1 (JCRB0172), and MCAS (JCRB0240). From the KCLB: SNU-840 (840). From RIKEN: OVK18 (RCB1903), JHOC-5 (RCB1520), JHOS-2 (RCB1521), JHOS-4 (RCB1678), JHOC-7 (RCB1688), JHOC-8 (RCB1723), JHOC-9 (RCB2226). From Sigma: COV434 (07071910-1VL), COV362 (07071910-1VL), OAW42 (85073102-1VL), COV644 (07071908-1VL), OV7 (96020764-1VL), A2780 (93112519-1VL), COV504 (07071902-1VL) and OV56 (96020759-1VL). Cell lines were authenticated by STR DNA typing. The Bin-67 SCCOHT line was provided by Barbara Vanderhyden at the Ottawa Hospital Research Institute.

In vitro compound treatment

Cultured cells were seeded into 6-well plates according to the cell densities below. Compound was diluted in DMSO (0.2%) and grown for 96 hours in 37°C and 5% CO_2. Cells were harvested by trypsinization, collected by centrifugation, rinsed with PBS before being flash-frozen on dry ice. Cells were seeded as follows, per well in a 6-well plate: Bin-67–$4E^5$, COV434–$2.5E^5$, OVK18–$3E^5$, TOV112D–$3E^4$, COV362–$1.5E^5$, JHOC-5–$6E^4$.

Western blot analysis

Cells or powdered tumor tissue were lysed in 1X RIPA buffer (Millipore, #20-188) with 0.1% SDS and Protease Inhibitor Cocktail tablet (Roche, #04693124001), and sonicated on ice before being spun at 4°C. Clarified supernatant was assayed for protein concentration by BCA (Pierce, #23225). Antibodies used for Western blotting include H3 (3638S), H3K27me3 (9733S), SMARCB1 (8745S), SMARCA2 (11966S), EZH2 (5246S), and β-actin (3700S), all from Cell Signaling Technology. SMARCA4 (ab110641) and vinculin (ab18058) were from Abcam. Imaging was performed using a LI-COR Odyssey, and changes in the target band were quantified by densitometry. Ratios between H3K27me3 and H3 were calculated and compound-treated samples were normalized to controls (DMSO or vehicle). IC_{50} values were determined by fitting the concentration-response data to a standard Langmuir isotherm equation (29).

H3K27me3 ELISA

Histones were isolated from tumors as previously described (30) and were prepared in coating buffer (0.05% BSA in PBS). H3K27me3 ELISAs were performed as previously described (3). The H3K27me3 (CST 9733S) and total H3 (CST 3638S) antibodies were used at 1:100 dilution and ratios for H3K27Me3 to total H3 were calculated.

In vitro long-term proliferation assay

Long-term proliferation assays were performed using the method previously described (30), with the following initial seeding densities: Bin-67 – $4E^3$, COV434 – $2.5E^3$, OVK18 $3E^3$, COV362 – $1.25E^3$, TOV112D – 312, PA-1 – 625, TYK-NU – 625, OAW42 – 312, JHOC-5 – 600 cells/well.

CRISPR pooled screen

A custom 6.5K sgRNA library, targeting over 600 epigenetic-related genes, was ordered from Cellecta. 195 cell lines (Supplementary Table S1) were screened as previously described (31, 32). Sensitivity was calculated using the Redundant siRNA activity (RSA) score, and is represented here as LogP, as previously described (33).

Data analysis

Cancer Cell Line Encyclopedia (CCLE) RNA seq data were downloaded from public sources. Two-dimensional hierarchical clustering was done in MATLAB R2015a using the "clustergram"

function from the Bioinformatics Toolbox (Mathworks). The clustering was done on the top 100, 500, and 1,000 most variable genes across 40 ovarian cell lines in the panel. Gene-expression signature scores were calculated as average expression across the signature genes.

Time course studies—Annexin and cell cycle

Cells were plated in 10-cm dishes and treated with 1 or 0.1 μmol/L tazemetostat (DMSO = 0.01%) for 3 to 21 days. A total of 1×10^5 harvested cells were plated in triplicate in 96-well format and stained with Millipore's Guava Nexin reagent (4500–0450) for 1 hour at room temperature. Percentages of cells undergoing apoptosis were measured using Millipore's Guava EasyCyte Flow Cytometer. For cell-cycle analysis, 5×10^5 cells were plated in a 96-well plate, washed once with PBS, and fixed overnight in ice-cold 70% ethanol at 4°C. Fixed cells were washed with PBS, then stained with Millipore's Guava Cell Cycle Reagent (4500–0220) and data obtained from EasyCyte Flow Cytometer.

***In vivo* xenograft studies**

All of the procedures related to animal handling, care, and the treatment in this study were performed according to the guidelines approved by the Institutional Animal Care and Use Committee (IACUC) of Shanghai Chempartner following the guidance of the Association for Assessment and Accreditation of Laboratory Animal Care (AAALAC). For the *in vivo* efficacy studies, there were 10 mice per dose group and each mouse was inoculated subcutaneously at the right flank. All cells were suspended in a 0.2 mL mixture of base media and Matrigel at 1:1 for tumor development. Bin-67 cells were inoculated at 5×10^6 cells/mouse and treatment began when the mean tumor sizes reached 146.08 mm^3 (28 days post-inoculation). COV434 cells were inoculated at 1×10^7 cells/mouse and treatment began when mean tumor sizes reached 158.88 mm^3 (20 days post-inoculation). TOV112D cells were inoculated at 5×10^6 cells/mouse and treatment began when the mean tumor size reached 128.13 mm^3 (day 14 post-inoculation). Mice were assigned into groups using a randomized block design. Tazemetostat or vehicle (0.5% methylcellulose + 0.1% TWEEN-80 in water) was administered orally BID at a dose volume of 125 or 500 mg/kg (COV434 for 28 days, TOV112D for 14 days) or 125, 250, or 500 mg/kg (Bin-67 for 19 days). Body weights were measured twice a week for the duration of the study. Tumor size was measured twice weekly in two dimensions using a caliper, and the volume was expressed in cubic millimeters. Animals were euthanized 3 hours post-final dose, with blood and tissues collected for analysis.

Results

Dual loss of SMARCA2 and SMARCA4 protein identifies three misclassified SCCOHT cell lines

It is known that SWI/SNF proteins can be inactivated in the absence of genomic mutations; hence, we tested a large panel of 37 ovarian cell lines of all major subtypes (serous, mucinous, endometrioid, clear cell, teratoma, SCCOHT, and unclassified/other) for protein levels of the commonly mutated or deleted SWI/SNF subunits ARID1A, SMARCB1 (INI1), SMARCA2, and SMARCA4 (Fig. 1A; Table 1; Supplementary Table S2). All cell lines had intact SMARCB1 protein, confirming that this protein is not commonly lost in ovarian cancer consistent with the genomic data (20). No significant differences in EZH2 or H3K27me3 levels were observed in select ovarian lines tested (Supplementary Fig. S1). *ARID1A* mutations have been reported to be more commonly observed in clear cell carcinoma and endometrioid carcinoma, though they are also present in other subtypes of ovarian cancers, and our protein data confirms this. Four of the 11 *ARID1A*-mutated cell lines were negative for ARID1A protein, suggesting that *ARID1A* mutations can lead to variable changes in protein levels. Interestingly, SMARCA2 and SMARCA4 expressions were absent in 16 (43%) and 6 (16%) cell lines respectively, indicating that these SWI/SNF components are commonly lost in ovarian cancer. Notably, four cell lines (11%) lacked expression of both SMARCA2 and SMARCA4 and these included the SCCOHT cell line Bin-67, the endometrioid cell lines TOV112D and OVK18, and the granulosa cell line COV434. We also examined SMARCA2 and SMARCA4 mRNA expression data for all ovarian cell lines using data from the Cancer Cell Line Encyclopedia (CCLE; ref. 34; which did not include Bin-67), and discovered that the TOV112D, COV434, and OVK18 cell lines displayed low to no expression of both SMARCA2 and SMARCA4, distinguishing them from the other ovarian cell lines (Fig. 1B and C). The lack of SMARCA4 mRNA and protein levels in these lines can be partially explained by loss of function mutations in *SMARCA4* (as reported by COSMIC and CCLE (refs. 34, 35; Table 1; Supplementary Table S2). Interestingly, these lines do not have any described coding mutations in *SMARCA2*, suggesting that the mechanism of *SMARCA2* inactivation is possibly through epigenetic silencing, as has been described previously to occur in SCCOHT and other indications (23, 24). As dual loss of SMARCA2 and SMARCA4 has been recently demonstrated to be a defining characteristic of SCCOHT within ovarian cancer (23, 24), these observations highly suggest that TOV112D, OVK18, and COV434 cell lines are derived from SCCOHT tumors that were misdiagnosed as a different ovarian cancer subtype. Interestingly, granulosa cell tumors, from which COV434 was derived, are categorized as a form of ovarian cancer that is known to mimic SCCOHT morphologically (36).

We performed hierarchical clustering of all ovarian cell lines within the CCLE dataset (which includes 3 of the 4 SCCCOHT cell lines TOV112D, COV434, and OVK18) and results showed that the three SCCOHT lines clustered together, consistent with a similar tumor cell of origin (Fig. 1B). To characterize further these SCCOHT cell lines, we performed transcriptome analysis of all ovarian cell lines within the CCLE dataset using the developmental and embryonic stem cell program signature that is characteristic of BAF-deficient sarcomas (ref. 37; Fig. 1D). When applying the BAF-deficient sarcoma gene signature to our analysis of the ovarian cell line panel, we found that 2 of the 3 SCCOHT cell lines, TOV112D and COV434, scored highest for this signature and together formed a single cluster, distinct from all other ovarian cell lines. Interestingly, OVK18 scored moderately for the BAF-deficient sarcoma gene signature; however, this cell line has a high mutational burden that may affect this analysis (38). These data suggest that SCCOHT cell lines may have expression patterns more similar to BAF-deficient sarcomas.

Tazemetostat potently inhibits SMARCA2- and SMARCA4-deficient ovarian cell lines

We tested the effect of EZH2 inhibition on this ovarian cell line panel with tazemetostat, a potent and selective EZH2 inhibitor currently in Phase 2 clinical trials (ref. 3; Fig. 2A and B; Table 1;

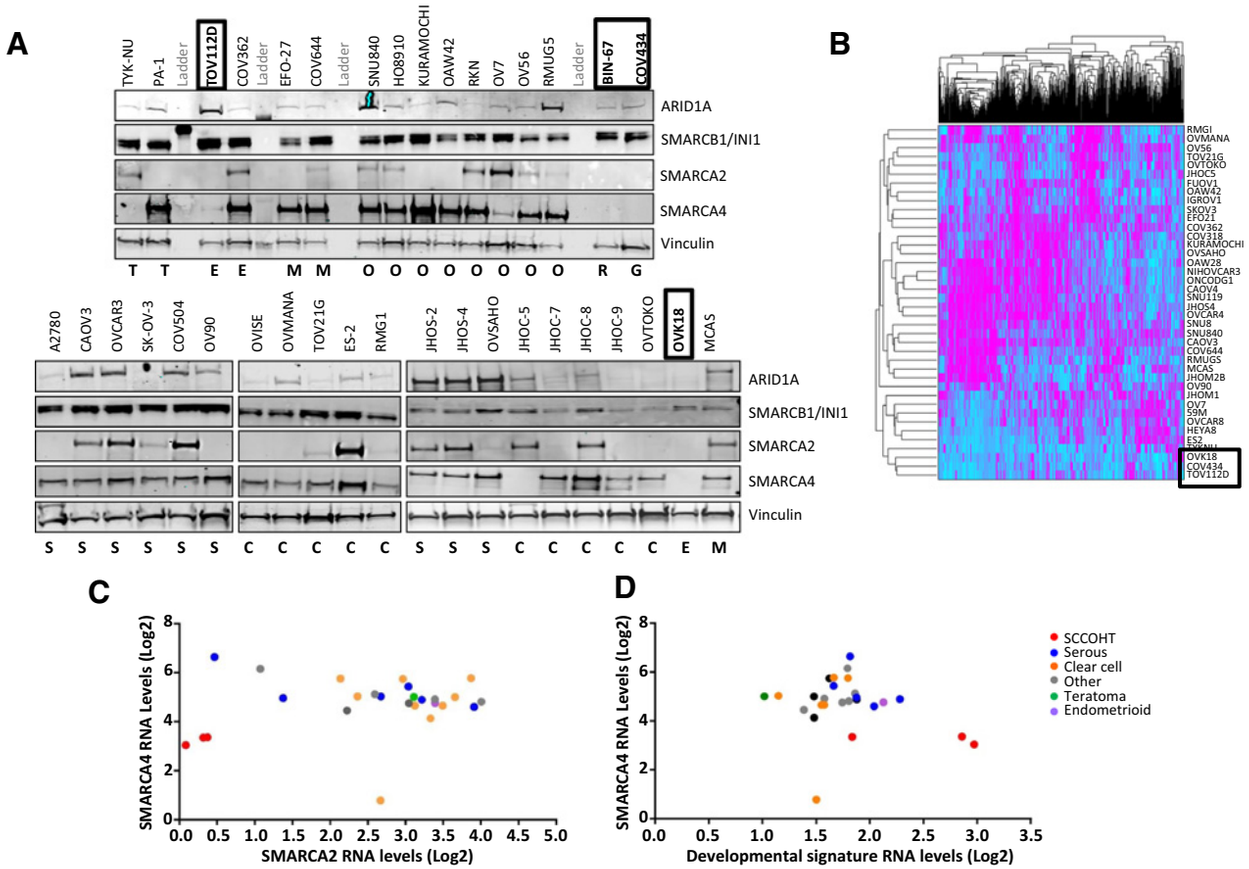

Figure 1.

A, Protein levels by Western blot analysis of SWI/SNF components (ARID1A, SMARCB1, SMARCA2, and SMARCA4) tested in 37 ovarian cancer cell lines. Subclasses are indicated underneath each lane as teratoma (T), endometrioid (E), mucosa (M), serous (S), clear cell (C), other/unknown (O), or SCCOHT (R). **B,** Two-dimensional hierarchical clustering of 500 most variable genes in all ovarian cell lines in CCLE (39) revealed clustering of three SCCOHT lines, OVK18, COV434, and TOV112D. The clustering was also performed on the top 100 and 1,000 most variable genes across the 40 ovarian cell lines and clustering was preserved. Cancer Cell Line Encyclopedia (CCLE) RNA seq data were downloaded from public sources. The data are displayed on the scale from −1.5 (blue) to 1.5 (pink) centered to the mean for each gene, where the gene expression values are $\log_2$ of the FPKM normalized RNA seq reads. **C,** Transcriptomic analysis of cell lines from **A** that also have data available from CCLE (26 in total) revealed that three cell lines, OVK18, TOV112D, and COV434 have no to very low levels of both SMARCA2 and SMARCA4 compared with all other ovarian cell lines within the panel. **D,** BAF-deficient sarcoma gene signature analysis revealed 2/3 SCCOHT lines, TOV112D and COV434, scored high and clustered away from the remaining cell line panel. The third SCCOHT cell line, OVK18, scored moderately.

Supplementary Table S2). As epigenetic inhibitors typically elicit antiproliferative effects with delayed kinetics relative to other targeted therapies, we used a long-term proliferation assay that quantifies cell growth over 15 days, at which point the evolution of compound potency for epigenetic inhibitors can be most fully realized (ref. 30; Fig. 2C; Supplementary Tables S3 and S4). Potent concentration-dependent antiproliferative effects of tazemetostat were observed in 5 of 36 ovarian cell lines in vitro ($IC_{50} \leq 1$ μmol/L). Of the remaining 31 cell lines, only 4 displayed IC_{50}'s of less than 10 μmol/L (teratoma cell line PA-1, serous cell lines CAOV-3 and COV504, and clear cell line TOV21G). Examination of the mutational burden of responding and nonresponding cell lines revealed that *ARID1A* mutational status does not correlate with sensitivity to EZH2 inhibition in these growth formats, contrary to what has been previously reported (refs. 39, 40; Fig. 2A). However, we note that the 4 SCCOHT cell lines, which lack both SMARCA2 and SMARCA4 protein expression, were preferentially sensitive to EZH2 inhibition (Fig. 2A and B). The antiproliferative effect of tazemetostat in these cell lines followed kinetics consistent with an EZH2 inhibitor (Fig. 2B; Supplementary Fig. S2A). Interestingly, those cell lines with loss of SMARCA4 or SMARCA2 individually (PA-1, OAW42, JHOC5, COV362, ES-2 or TYK-NU) were far less sensitive to tazemetostat, suggesting that loss of both redundant (ATPase-containing) SWI/SNF subunits is required to confer sensitivity to EZH2 inhibition. Long-term proliferation effects were also tested using a chemically distinct EZH2 inhibitor (41) in a select number of ovarian cell lines and preferential sensitivity in SCCOHT lines was also observed, confirming that phenotypic effects are due to EZH2 inhibition (Supplementary Fig. S2B).

To exclude the possibility that the sensitivity or resistance to tazemetostat was due to differential inhibition of EZH2 activity, the potency of tazemetostat for inhibition of global H3K27me3

Table 1. Characterization of ovarian cell lines

		SMARCA2		SMARCA4		ARID1A		Tazemetostat day 4 H3K327me3 IC_{50} (μmol/L)	Tazemetostat day 15 Proliferation IC_{50} (μmol/L)
Cell line	**Subtype**	**Mutation**	**Protein**	**Mutation**	**Protein**	**Mutation**	**Protein**		
Bin-67	SCCOHT	ND	**Absent**	c.2438+1G>A c.2439−2A>T	**Absent**	ND	Present	0.008	0.29
COV434	SCCOHT	ND	**Absent**		**Absent**	G1255E	Present	0.008	0.073
TOV112D	SCCOHT		**Absent**	p.L639fs*7	**Absent**		Present	0.010	0.34
OVK18	SCCOHT		**Absent**	p.P109fs*194	**Absent**	p.Y592fs*27	**Absent**	0.032	0.86
TYK-NU	Teratoma		Present		**Absent**		Present	0.016	>10
JHOC5	Clear cell/ endometrioid	ND	Present		**Absent**		Present	0.001	>10
OAW42	Other (epithelial, cystoadenocarcinoma)		**Absent**		Present	p.P559fs*63, p.A1119fs*4	Present	0.007	>10
PA-1	Teratoma		**Absent**		Present		Present	0.04	5.9
COV362	Endometrioid	ND	Present		Present		Present	0.015	>10
ES-2	Clear cell/endometrioid		Present		Present		Present	Not done	>10

NOTE: Information is listed for each line on: genetic status of SWI/SNF protein components, presence or absence of SWI/SNF protein component identified by Western blot analysis, tazemetostat day 4 H3K27me3 IC_{50} (μmol/L), and tazemetostat long-term proliferation (LTP) day 15 IC_{50} (μmol/L). All mutations are reported by CCLE or COSMIC. ND, no data available; empty cells indicate WT gene status. Where multiple subtypes are indicated, classification varied depending on publication.

production was tested in the four sensitive SCCOHT cell lines (Bin-67, OVK18, COV434, and TOV112D) and five insensitive ovarian cancer cell lines (COV362, JHOC-5, TYK-NU, PA-1 and OAW42). As expected, all cell lines tested showed similar magnitude and potency of concentration-dependent methyl mark inhibition (Fig. 2D; Supplementary Fig. S3). In sensitive cell lines the antiproliferative effect was observed at doses consistent with EZH2 inhibition as measured by methyl mark reduction. EZH2 inhibition was also maximally achieved in non-responding cell lines without antiproliferative effect. These data suggest that only cell lines with the dual loss of SMARCA2 and SMARCA4 are critically dependent on EZH2 (Table 1; Supplementary Table S2). Because loss of SMARCA2 protein occurs in the absence of any gene alterations and is hypothesized to be posttranscriptionally regulated, we tested whether tazemetostat could upregulate SMARCA2 expression. Indeed, in SCCOHT cell lines, tazemetostat treatment led to time-dependent increases in SMARCA2 expression (Fig. 2E).

Apoptosis and cell-cycle progression were examined following tazemetostat treatment in two SCCOHT lines (COV434 and Bin-67) and the serous line JHOS-2 (Fig. 3; Supplementary Tables S5 and S6). COV434 cells showed an increase in the percentage of cells in sub-G_1 phase and a concomitant reduction in G_2 phase after 3 days and continuing through to day 14, consistent with an increase in apoptotic cells measured by Annexin staining. Bin-67 cells showed a more modest increase in the percentage of sub-G_1 cells and this was consistent with apoptotic events observed as early as day 4. In contrast, the cell line JHOS-2 (wild-type for both *SMARCA2* and *SMARCA4*) treated with tazemetostat did not show any cell-cycle changes or apoptotic events, consistent with the lack of antiproliferative effects following EZH2 inhibition. These data suggest that the mechanism of cell death in SCCOHT lines is through induction of apoptosis.

CRISPR pooled screen identifies SCCOHT cell line COV434 as sensitive to EZH2 knockout

It has been reported that some tumors with SWI/SNF mutations are dependent on the EZH2 protein itself as a scaffold, but not its catalytic activity (40). Therefore, as we identified ovarian cell lines with loss of expression or mutation in individual SWI/SNF subunits that were insensitive to tazemetostat inhibition of EZH2 catalytic activity, we sought to determine whether they were otherwise sensitive to knockout of EZH2 through CRISPR/Cas9-mediated gene knockout. CRISPR/Cas9 pooled screening is a high-throughput method to evaluate 100s to 1000s of genes in a single experiment with high data quality (31, 32). Briefly, a large population of cells is infected with a pooled library of barcoded sgRNA guides to genes of interest. For proliferation-based screens, the barcode/sgRNA representation is measured at the start and end of the experiment by sequencing of genomic DNA, and the relative enrichment/decrease in CRISPR sgRNAs identifies genes for which knockout alters proliferation rate. We generated a custom CRISPR lentiviral library with 6,500 small guide RNAs targeting over 600 epigenetic genes, and screened it against 195 cell lines (Supplementary Table S1) over a time course of up to 40 days. We calculated the dependency on each gene as previously described for shRNA pooled screening, using the Redundant siRNA Algorithm (RSA; refs. 33, 42).

The screen performed well, as exemplified by our control pan-essential target PLK1 (polo-like kinase 1), which shows dependency in nearly all cell lines (Supplementary Fig. S4A), and our negative control nontargeting sgRNAs, which show no proliferation effects (six representative negative control sgRNAs shown in Supplementary Fig. S4B). We included KRas as a positive control in our CRISPR/Cas9 library, and as expected observed that sensitivity to KRas knockout was highly correlated with KRas mutations (Fig. 4A). We also confirmed that *SMARCA4* null or mutant cells, including A549 and NCIH1299 lung cancer cell lines, are sensitive to *SMARCA2* knockout as previously reported (refs. 43, 44; Fig. 4B). This indicates that the screen performs well and can identify known epigenetic and nonepigenetic dependencies as well as known pan-essential genes.

Our 195 cell line collection included 13 ovarian cell lines, one of which was COV434, which we later identified to be of SCCOHT origin based on dual loss of SMARCA2 and SMARCA4. The other 13 ovarian cell lines included in the screen are highlighted in

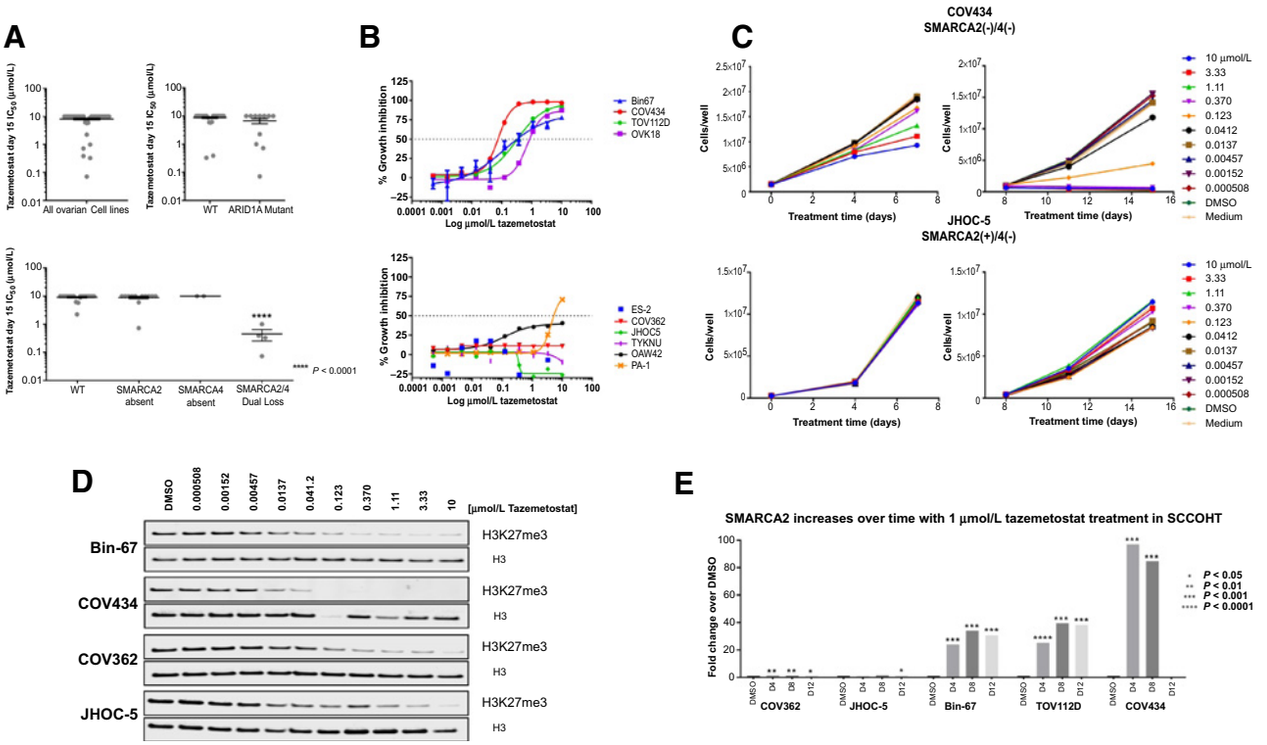

Figure 2.

A, Thirty seven ovarian cell lines shown in Fig. 1 were tested in long-term proliferation assays with tazemetostat. IC_{50}s between 0.073 and >10 µmol/L were observed. Cell lines with loss of both SMARCA2 and SMARCA4 were most sensitive to tazemetostat (IC_{50} values of less than 1 µmol/L, $P < 0.0001$). LTP IC_{50} values were not significantly different between ARID1A WT and ARID1A mutated cell lines (top right, $P > 0.05$). Significance determined using the two-tailed unpaired T test. **B,** Dose-dependent inhibition of cell growth is observed upon tazemetostat treatment in four SMARCA2-deficient and SMARCA4-deficient cell lines, but not in SMARCA4-deficient JHOC-5 and TYKNU, SMARCA2-deficient PA-1 and OAW42, or SMARCA2 and SMARCA4 WT cell line ES-2 or COV362 (technical replicates, $n = 3$). **C,** Representative growth curve plots from a SMARCA2-deficient and SMARCA4-deficient SCCOHT cell line (COV434) and a SMARCA2 WT and SMARCA4-deficient cell line (JHOC-5). Antiproliferative effects observed in SCCOHT cell lines treated with tazemetostat. Day 15 IC_{50} values are shown in Table 1 (technical replicates, $n = 3$). Significance determined using the two-tailed paired T test (Supplementary Tables S3 and S4). **D,** Shown are representative H3K27me3 Western blots in SMARCA2 and SMARCA4 dual loss SCCOHT lines (Bin-67, COV434), a SMARCA4-deficient cell line (JHOC-5), and a SMARCA2 and SMARCA4 wild-type cell line (COV362). H3K27me3 IC_{50} values are shown in Table 1. **E,** SMARCA2 mRNA was upregulated upon tazemetostat treatment in SCCOHT and not in non-SCCOHT cell lines over time. *, day 12 sample too small to test. Significance determined using two-tailed paired T test.

Fig. 4C. The SCCOHT cell line, COV434, was the only ovarian cell line to be sensitive to EZH2 knockout and was one of the most sensitive cell lines across all the cell lines screened (Fig. 4C). Two EZH2-insensitive cell lines (TYKNU and JHOC-5) with low SMARCA4 expression were instead sensitive to *SMARCA2* knockout, similar to what has been previously reported (Fig. 4B). These data indicate that inhibition of EZH2 catalytic activity by tazemetostat displays the same effects as genetic knockout of EZH2, arguing against a non-enzymatic scaffolding effect of EZH2 in these cell lines.

Next, we examined whether knockout of individual SWI/SNF protein components in an insensitive cell line can induce sensitivity to EZH2 inhibition. To achieve this, six ovarian cell lines were treated with or without tazemetostat and screened with our custom CRISPR pooled library (Fig. 4D; Supplementary Table S7). No consistent changes in sensitivity were observed in any of the tested cell lines following tazemetostat treatment when a single SWI/SNF component or when EZH2 was knocked out. As can be seen no synergy was observed between EZH2 knockout and tazemetostat treatment, further strengthening the argument that antiproliferative effects of tazemetostat in SCCOHT are mediated through EZH2 inhibition. Interestingly, *SMARCA2* knockout in three cell lines with low SMARCA4 expression, (OVISE, RMGI, OV90) did not lead to sensitivity following tazemetostat treatment. This suggests that the sensitivity of SCCOHT lines to EZH2 inhibition cannot be phenocopied by ablating *SMARCA2* in other ovarian cancer subtypes harboring low SMARCA4 expression. Thus, the cell-of-origin and other cell-intrinsic factors contribute to EZH2 essentiality in SCCOHT.

Antitumor effects observed in tazemetostat-treated SCCOHT xenografts

To ensure that the observed growth effects are not limited to two-dimensional culture conditions we treated cell line mouse xenografts with tazemetostat to test three-dimensional *in vivo* effects. Tazemetostat efficacy studies were performed in BALB/c nude mice bearing subcutaneous Bin-67, COV434, and TOV112D xenografts (Fig. 5; Supplementary Fig. S5). In the COV434 and TOV112D models, animals were dosed orally in three groups (vehicle, 125 and 500 mg/kg), twice daily (BID) for 28 days in the COV434 model and for 14 days in the TOV112D model. In the

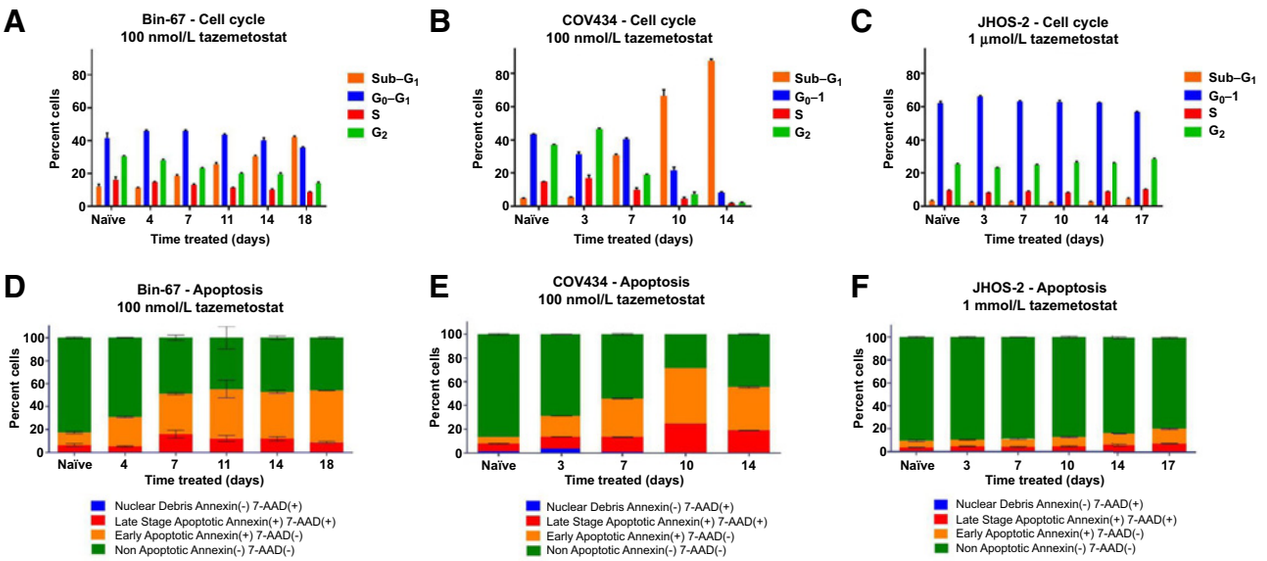

Figure 3.

Time course treatment of ovarian cell lines with tazemetostat, treated cells stained with propidium iodide show G_0–G_1 arrest in SCCOHT lines Bin-67 (**A**) and COV434 (**B**) after 14 days of treatment and also a significant increase in sub-G_1 events, indicating high rates of cell death. SMARCA2 and SMARCA4 WT ovarian line JHOS-2 was unaffected by treatment (**C**). An increase in apoptotic events as measured by annexin positive staining was observed in Bin-67 (**D**) and COV434 (**E**) but not in JHOS-2 (**F**). Cell-cycle data: orange represents sub G_1 events, blue represents G_0–G_1 events; red, S (synthesis) events; green, G_2 events. Apoptosis data: blue, annexin (−)/7-AAD (+) events; red, annexin (+)/7-AAD (+); orange, annexin (+)/7-AAD (−); green, Annexin (−)/7-AAD (−); all data points represent $n = 1$. Significance determined using two-tailed paired *t* test (Supplementary Tables S5 and S6).

Bin-67 model, animals were dosed orally in four groups (vehicle, 125, 250, and 500 mg/kg), twice daily for 18 days. All three studies reached endpoint when the vehicle tumors reached approximately 2,000 mm^3. After 28 days of dosing in the COV434 model one-half of the mice in the 500 mg/kg dose group were euthanized to collect blood and tissues while the remaining animals continued on the study to monitor for tumor regrowth. All dose groups in the tazemetostat-treated Bin-67 and TOV112D xenografts were euthanized to collect blood and tissues after 18 and 14 days of dosing respectively. Tumors showed statistically significant differences in volume compared with vehicle after 14 days in the TOV112D model, after 18 days in the Bin-67 model, and after 28 days in the COV434 model (Fig. 5; Supplementary Fig. S5). Bin-67 xenografts were analyzed on day 18 and showed 56% tumor growth inhibition (TGI) and 87% TGI in the 125 and 250 mg/kg dose groups respectively (Fig. 5A). Tumors in the 500 mg/kg dose group showed regressions in all 10 animals with an average tumor volume of 41 mm^3. TOV112D xenografts are fast growing and as a result the study completed on day 14. The 125 mg/kg and 500 mg/kg dose groups showed statistically significant TGI of 28% and 35%, respectively, on day 14 (Supplementary Fig. S5). On day 28 COV434 xenografts from the 125 mg/kg dose group showed 74% TGI, whereas the tumors in the 500 mg/kg dose group showed complete regressions with 7 of the 8 animals having unmeasurable tumors. Regrowth was not observed for 28 days after dose cessation (Fig. 5C). In both models, tazemetostat was well tolerated with minimal bodyweight loss and no other clinical observations (Supplementary Fig. S6). Dose-dependent systemic exposure of tazemetostat was measured in plasma collected 5 minutes prior or 3 hours after final dose for all models (Supplementary Fig. S7). Measurement of H3K27me3 levels in tumors harvested at study endpoints showed robust inhibition that correlated with antitumor activity (Fig. 5B and D; Supplementary Fig. S5C). These data, combined with the *in vitro* proliferation data, demonstrate that EZH2 inhibition by tazemetostat elicits potent antitumor activity in SCCOHT.

Discussion

The data reported here describe, for the first time, the oncogenic dependency of dual SMARCA2- and SMARCA4-deficient SCCOHT preclinical models on PRC2 activity. Given the rarity of this subtype of ovarian cancer, as well as the lack of SCCOHT-specific markers, this disease has been largely understudied and very difficult to diagnose. The identification of SMARCA2 and SMARCA4 dual loss as a defining feature of SCCOHT has advanced not only the biological understanding of this tumor type but has improved the diagnosis and clinical management of the disease. On the basis of the SMARCA2 and SMARCA4 dual loss, we were able to confirm that the Bin-67 cell line is of SCCOHT origin and as well identify three additional SCCOHT cell lines from our 37 ovarian cell line panel. These three misattributed cell lines have been used in numerous published studies, namely COV434 which has been reported to be only one of two available immortalized cell lines representing human granulosa cell tumors. This further emphasizes the difficulty in diagnosing SCCOHT; this finding also cautions that care must be taken when working with cell lines of unclear attribution. We showed here that SCCOHT cell lines are uniquely sensitive to tazemetostat treatment among other types of ovarian cancer in long-term proliferation assays. We further showed that tazemetostat evoked significant antitumor effects in xenograft models of SCCOHT cell lines. In addition to small-molecule inhibitor data, our functional genomics studies confirm that SCCOHT is

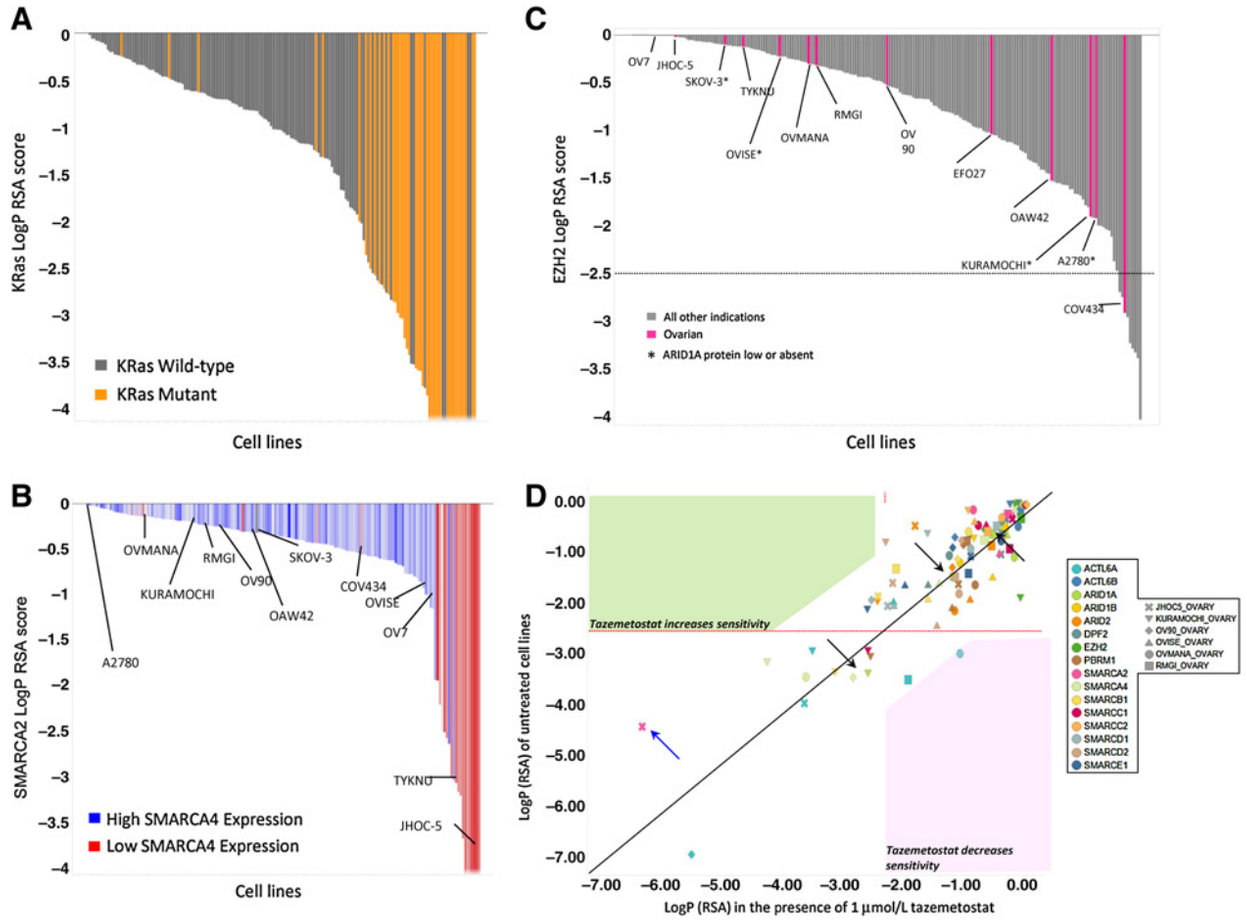

Figure 4.

A, CRISPR pooled screen data from 170 cell lines for which mutation data are available in CCLE. On the *y*-axis is sensitivity (LogP RSA) to KRas knockout. Cell lines are colored by KRas mutations: gray, wild type; orange, mutant. **B,** CRISPR pooled screen data from 170 cell lines for which microarray expression data are available in CCLE. On the *y*-axis is sensitivity (RSA LogP) to SMARCA2 knockout. Cell lines are colored by SMARCA4 expression: blue, high SMARCA4 expression; red, low SMARCA4 expression. Cell lines that are sensitive to SMARCA2 knockout tend to have low SMARCA4 expression, including two ovarian cell lines (TYKNU and JHOC-5). **C,** CRISPR-pooled screen data from 195 cell lines, including 13 ovarian cell lines, one of which we identified to be of SCCOHT origin based on dual loss of SMARCA2 and SMARCA4. This cell line, COV434, was the only ovarian cell line to be sensitive to EZH2 knockout. The *y*-axis is the LogP of the RSA score, which represents the sensitivity of knockout to EZH2. A cutoff of −2.5 for the LogP was used as this delineates KRas-sensitive mutant cells in **A**. Pink, ovarian cell lines; gray, all other indications. *, indicates absent or low levels of ARID1A protein by Western blot analysis. **D,** Six ovarian cell lines were treated with or without 1 µmol/L tazemetostat and screened with an epigenetic-centric CRISPR pooled library. The graph shows the sensitivity (RSA LogP) score for each cell line and each SWI/SNF component or EZH2 with or without treatment. The *y*-axis values represent scores in the absence of tazemetostat treatment, and the *x*-axis represent scores in the presence of tazemetostat treatment. Data are colored by gene and shaped by cell line. The pink and green area denote where data would fall if EZH2 inhibition led to a decrease or increase in sensitivity, respectively. Three cell lines with low expression of SMARCA2 (OVISE, RMGI, and OV90) are marked by black arrows. One cell line, JHOC-5 (blue arrow), which has low SMARCA4 expression, is sensitive to knockout of SMARCA2 both in the presence and absence of EZH2 inhibition. The solid line is $x = y$, and the dotted red lines represent sensitivity cut-off values. Data are an average of two time points.

dependent on EZH2 activity, as a single SCCOHT cell line was the only ovarian cancer line sensitive to *EZH2* gene ablation in CRISPR pooled screen.

It has been reported that SCCOHT shares similarities with malignant rhabdoid tumors (MRT) despite having mutations in different SWI/SNF complex members (20, 21, 27). The molecular, histopathological, and clinical commonalities between SCCOHT and rhabdoid tumors have led to the suggestion that SCCOHT be reclassified as "malignant rhabdoid tumor of the ovary" (MRTO) (20, 27). We previously reported the dependency of MRT on PRC2 activity using preclinical models that showed antiproliferative effects upon tazemetostat treatment (3) and here we report for the first time the same sensitivity to EZH2 inhibition of SCCOHT preclinical models. In this study, we report data to support further the existence of a class of rhabdoid-like tumors that not only represent a mesenchymal stem cell-like group of cancers that have misregulated SWI/SNF function (characterized by SWI/SNF loss of function mutations) but that are also dependent on PRC2 activity. This specific tumor class also shares clinical and histopathological features and has been found to carry a BAF-deficient sarcoma gene signature that is represented by developmental and embryonic stem cell programs (37). It is important to note that loss of SWI/SNF components alone does not predict

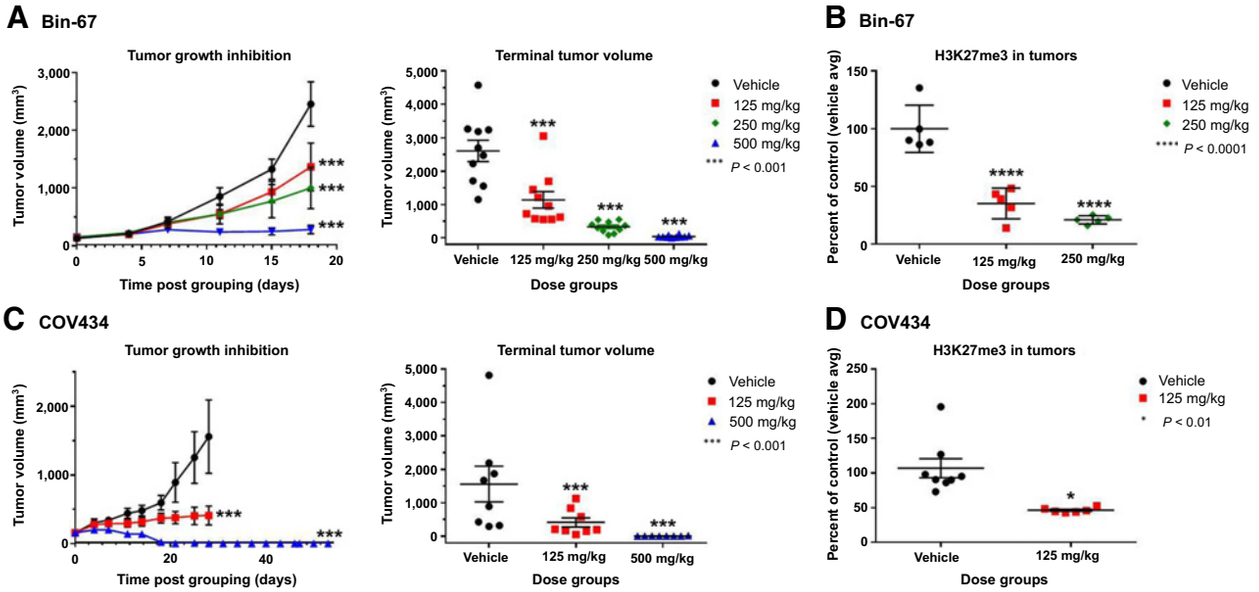

Figure 5.

A–D, *In vivo* xenograft tumors from SCCOHT lines were dosed with tazemetostat for 18 days (Bin-67, **A** and **B**) or 28 days (COV434, **C** and **D**). Tumors showed statistically significant (two-tailed paired *t* test) differences in volume compared with vehicle after 18 and 28 days in the Bin-67 and COV434 xenograft models, respectively. After day 28, a portion of the COV434 xenograft mice from the 500 mg/kg cohort were retained to monitor for tumor regrowth while under no treatment. EZH2 target inhibition was assessed by H3K27me3 levels in xenograft tissue collected on day 18 for Bin-67 (**B**) and day 28 for COV434 (**D**). Each point represents the ratio of H3K27me3 to total H3 from the tumor of a single animal as measured by ELISA. The tumors from the 500 mg/kg dose groups in both models were too small to sample and therefore methyl mark data could not be generated.

sensitivity to EZH2 inhibition. *In vitro* data demonstrated that ovarian cell lines with *ARID1*A mutations did not display antiproliferative effects upon tazemetostat treatment nor show sensitivity to *EZH2* knockout in our CRISPR pooled screen. This is in contrast with previous reports that showed *in vitro* and *in vivo* sensitivity of *ARID1A*-mutated lines upon treatment with GSK126, another EZH2 inhibitor, and EZH2 shRNA knockdown (39, 40). Given the known off-target effects that accompany RNAi methods, CRISPR knockout is more effective and specific for interpreting gene knockout phenotypes. Therefore, our inhibitor data along with our CRISPR data suggest that at least *in vitro*, *ARID1A*-mutated cell lines may not be as sensitive to EZH2 loss. An area of high interest is therefore to test the contribution of the tumor microenvironment in *ARID1A*-mutated *in vivo* models upon tazemetostat treatment. The cancer cell-of-origin appears to be a critical codeterminant of dependence on EZH2 activity; transcriptome analysis performed on a select number of SWI/SNF altered primary tumors revealed that SMARCA4- or INI1-deficient rhabdoid-like tumors clustered together and away from SMARCA4-deficient lung tumors, a more epithelial and more differentiated type of tumor (37). In addition, data from our CRISPR pooled screen show that knocking out *SMARCA4* in a SMARCA2 low-expressing cell line (and vice versa) does not sensitize the cells to tazemetostat treatment further supporting the importance of the cell of origin. During SCCOHT oncogeneis, cells likely become dependent on EZH2 activity early in tumorgenesis, as supported by the low mutational burden of rhabdoid tumors deficient of SMARCA2 and SMARCA4/INI1 (19, 20, 22). This further suggests that engineering a synthetic lethal reliance on EZH2 via knockout of the second ATPase is not feasible in a tumor that is already not a dependent EZH2 cell line (*e.g.*, a non-SCCOHT ovarian tumor). In the case of epigenetic targets which modulate global transcriptional regulation and state, the path by which a cell arrives at a malignant state is likely to determine whether a synthetic lethal relationship exists (which will likely occur with many epigenetic targets). This is likely distinct from pathway synthetic lethality which is agnostic to cell-of-origin.

SMARCA2 and SMARCA4 are mutually exclusive ATPase subunits of the SWI/SNF complex. Studies in other cancer types which also show dual loss (e.g., NSCLC) have surprisingly shown that the SWI/SNF complex can still form in the absence of any ATPase subunit (43). It remains to be seen whether a residual complex forms in SCCOHT and if it retains any remodeling activity. Interestingly, SMARCA2 loss has been observed in numerous other cancer cell lines and primary tissues though genetic mutations are rare, suggesting epigenetic or post-transcriptional silencing events (45). Interestingly, a study showed that the histone deacetylase inhibitor trichostatin A was able to reactivate the expression of SMARCA2 in a SMARCA2-low SCCOHT cell line. The same study showed that reexpression of either ATPase in SCCOHT cell lines was able to inhibit cell growth emphasizing the importance of SMARCA2 and SMARCA4 dual loss in SCCOHT (24). We also observed upregulation of SMARCA2 upon tazemetostat treatment in SCCOHT cell lines (Fig. 2E). Further studies are underway not only to determine the role of SMARCA2 upregulation in cell death in SCCOHT but also to understand the functional consequences of SWI/SNF mutations for both complex activity as well as downstream pathway alterations.

These preclinical data suggest that tazemetostat may have therapeutic benefit in patients with MRT and SCCOHT. Indeed, we reported the first clinical activity of an EZH2 inhibitor in patients with INI-deficient MRT and SMARCA4-deficient SCCOHT in our Phase 1, first-in-human study (E7438-G000-001, NCT01897571), testing the effects of tazemetostat in INI1-deficient and SMARCA4-deficient relapse and/or refractory solid tumors (46). Within this study of 51 patients (30 solid tumor and 21 non-Hodgkin's lymphoma) immunohistochemistry of tumor tissue identified five INI1-deficient MRT patients and two SMARCA4-deficient SCCOHT patients. As reported by Ribrag and colleagues (46) responses observed in patients with MRT after 8 weeks of treatment included one complete response (CR), one partial response (PR), two stable disease (SD), and one progressive disease (PD). Clinical responses observed in patients with SCCOHT after 8 weeks of treatment included one PR and one SD. Time on study for these patients ranged from 11 to 65+ weeks. It is important to note that patients with rhabdoid tumors have a very aggressive disease course, are resistant to chemotherapy, and have a survival rate of <25% with a mean time to death of <9 months. Thus, the observation of tumor regression and even sustained disease stabilization in patients with this tumor appears to be of notable clinical benefit.

In summary, we report a novel dependence on PRC2 activity in the rhabdoid-like tumor of the ovary, SCCOHT, similar to that seen in MRT. We observed therapeutic benefit of EZH2 inhibition in patients with SCCOHT, as predicted from the preclinical data presented in this report. Identifying additional rhabdoid-like tumors in other tissue classes is currently an active area of investigation as they represent an indication potentially amenable to treatment with an EZH2 inhibitor as monotherapy.

Disclosure of Potential Conflicts of Interest

M. Roche has ownership interest (including patents) in Epizyme. P. Ho is a chief medical officer at Epizyme and is a consultant/advisory board member for Lilly Asia Ventures. R.A. Copeland is a consultant at Synergy Partners, has ownership interest (including patents) in Epizyme, and is a consultant/advisory board member for Mersana and Raze Therapeutics. R. Chesworth has ownership interest (including patents) in Epizyme. J.J. Smith has ownership interest (including patents) in Epizyme stock options. Heike Keilhack has ownership interest (including patents) in Epizyme Stock. No potential conflicts of interest were disclosed by the other authors.

Authors' Contributions

Conception and design: E. Chan-Penebre, K. Armstrong, A. Drew, A.R. Grassian, S.K. Knutson, K. Kuplast-Barr, R.A. Copeland, J.J. Smith, H. Keilhack, S.A Ribich

Development of methodology: E. Chan-Penebre, K. Armstrong, A. Drew, A.R. Grassian, S.K. Knutson, K. Kuplast-Barr

Acquisition of data (provided animals, acquired and managed patients, provided facilities, etc.): E. Chan-Penebre, K. Armstrong, A. Drew, A.R. Grassian, S.K. Knutson, K. Kuplast-Barr, J. Campbell

Analysis and interpretation of data (e.g., statistical analysis, biostatistics, computational analysis): E. Chan-Penebre, K. Armstrong, A. Drew, A.R. Grassian, I. Feldman, K. Kuplast-Barr, R.A. Copeland, S.A Ribich

Writing, review, and/or revision of the manuscript: E. Chan-Penebre, K. Armstrong, A. Drew, A.R. Grassian, K. Kuplast-Barr, M. Roche, P. Ho, R.A. Copeland, R. Chesworth, S.A Ribich

Administrative, technical, or material support (i.e., reporting or organizing data, constructing databases): K. Armstrong

Study supervision: K. Kuplast-Barr, R. Chesworth, J.J. Smith, S.A Ribich

The costs of publication of this article were defrayed in part by the payment of page charges. This article must therefore be hereby marked *advertisement* in accordance with 18 U.S.C. Section 1734 solely to indicate this fact.

Received October 14, 2016; revised November 2, 2016; accepted February 23, 2017; published OnlineFirst March 14, 2017.

References

1. Chase A, Cross NC. Aberrations of EZH2 in cancer. Clin Cancer Res 2011;17:2613–8.
2. McCabe MT, Ott HM, Ganji G, Korenchuk S, Thompson C, Van Aller GS, et al. EZH2 inhibition as a therapeutic strategy for lymphoma with EZH2-activating mutations. Nature 2012;492:108–12.
3. Knutson SK, Warholic NM, Wigle TJ, Klaus CR, Allain CJ, Raimondi A, et al. Durable tumor regression in genetically altered malignant rhabdoid tumors by inhibition of methyltransferase EZH2. Proc Natl Acad Sci U S A 2013;110:7922–7.
4. Kawano S, Grassian AR, Tsuda M, Knutson SK, Warholic NM, Kuznetsov G, et al. Preclinical evidence of anti-tumor activity induced by EZH2 inhibition in human models of synovial sarcoma. PLoS ONE 2016;11: e0158888.
5. LaFave LM, Beguelin W, Koche R, Teater M, Spitzer B, Chramiec A, et al. Loss of BAP1 function leads to EZH2-dependent transformation. Nat Med 2015;21:1344–9.
6. Knutson SK, Kawano S, Minoshima Y, Warholic NM, Huang KC, Xiao Y, et al. Selective inhibition of EZH2 by EPZ-6438 leads to potent antitumor activity in EZH2-mutant non-Hodgkin lymphoma. Mol Cancer Ther 2014;13:842–54.
7. Knutson SK, Wigle TJ, Warholic NM, Sneeringer CJ, Allain CJ, Klaus CR, et al. A selective inhibitor of EZH2 blocks H3K27 methylation and kills mutant lymphoma cells. Nat Chem Biol 2012;8:890–6.
8. Kadoch C, Crabtree GR. Mammalian SWI/SNF chromatin remodeling complexes and cancer: mechanistic insights gained from human genomics. Sci Adv 2015;1:e1500447.
9. Kadoch C, Hargreaves DC, Hodges C, Elias L, Ho L, Ranish J, et al. Proteomic and bioinformatic analysis of mammalian SWI/SNF complexes identifies extensive roles in human malignancy. Nat Genet 2013;45:592–601.
10. Helming KC, Wang X, Roberts CW. Vulnerabilities of mutant SWI/SNF complexes in cancer. Cancer Cell 2014;26:309–17.
11. Versteege I, Sevenet N, Lange J, Rousseau-Merck MF, Ambros P, Handgretinger R, et al. Truncating mutations of hSNF5/INI1 in aggressive paediatric cancer. Nature 1998;394:203–6.
12. Ginn KF, Gajjar A. Atypical teratoid rhabdoid tumor: current therapy and future directions. Front Oncol 2012;2:114.
13. Wilson BG, Wang X, Shen X, McKenna ES, Lemieux ME, Cho YJ, et al. Epigenetic antagonism between polycomb and SWI/SNF complexes during oncogenic transformation. Cancer Cell 2010;18:316–28.
14. Su L, Sampaio AV, Jones KB, Pacheco M, Goytain A, Lin S, et al. Deconstruction of the SS18-SSX fusion oncoprotein complex: insights into disease etiology and therapeutics. Cancer Cell 2012;21: 333–47.
15. Shen JK, Cote GM, Gao Y, Choy E, Mankin HJ, Hornicek FJ, et al. Targeting EZH2-mediated methylation of H3K27 inhibits proliferation and migration of Synovial Sarcoma in vitro. Sci Rep 2016;6:25239.
16. Matsubara D, Kishaba Y, Ishikawa S, Sakatani T, Oguni S, Tamura T, et al. Lung cancer with loss of BRG1/BRM, shows epithelial mesenchymal transition phenotype and distinct histologic and genetic features. Cancer Sci 2013;104:266–73.
17. Reisman DN, Sciarrotta J, Wang W, Funkhouser WK, Weissman BE. Loss of BRG1/BRM in human lung cancer cell lines and primary lung cancers: correlation with poor prognosis. Cancer Res 2003;63:560–6.
18. Yoshimoto T, Matsubara D, Nakano T, Tamura T, Endo S, Sugiyama Y, et al. Frequent loss of the expression of multiple subunits of the SWI/SNF

complex in large cell carcinoma and pleomorphic carcinoma of the lung. Pathol Int 2015;65:595–602.
19. Jelinic P, Mueller JJ, Olvera N, Dao F, Scott SN, Shah R, et al. Recurrent SMARCA4 mutations in small cell carcinoma of the ovary. Nat Genet 2014;46:424–6.
20. Witkowski L, Carrot-Zhang J, Albrecht S, Fahiminiya S, Hamel N, Tomiak E, et al. Germline and somatic SMARCA4 mutations characterize small cell carcinoma of the ovary, hypercalcemic type. Nat Genet 2014;46:438–43.
21. Ramos P, Karnezis AN, Hendricks WP, Wang Y, Tembe W, Zismann VL, et al. Loss of the tumor suppressor SMARCA4 in small cell carcinoma of the ovary, hypercalcemic type (SCCOHT). Rare Dis 2014;2:e967148.
22. Ramos P, Karnezis AN, Craig DW, Sekulic A, Russell ML, Hendricks WP, et al. Small cell carcinoma of the ovary, hypercalcemic type, displays frequent inactivating germline and somatic mutations in SMARCA4. Nat Genet 2014;46:427–9.
23. Jelinic P, Schlappe BA, Conlon N, Tseng J, Olvera N, Dao F, et al. Concomitant loss of SMARCA2 and SMARCA4 expression in small cell carcinoma of the ovary, hypercalcemic type. Mod Pathol 2016;29: 60–6.
24. Karnezis AN, Wang Y, Ramos P, Hendricks WP, Oliva E, D'Angelo E, et al. Dual loss of the SWI/SNF complex ATPases SMARCA4/BRG1 and SMARCA2/BRM is highly sensitive and specific for small cell carcinoma of the ovary, hypercalcaemic type. J Pathol 2016;238:389–400.
25. Young RH, Oliva E, Scully RE. Small cell carcinoma of the ovary, hypercalcemic type. A clinicopathological analysis of 150 cases. Am J Surg Pathol 1994;18:1102–16.
26. Callegaro-Filho D, Gershenson DM, Nick AM, Munsell MF, Ramirez PT, Eifel PJ, et al. Small cell carcinoma of the ovary-hypercalcemic type (SCCOHT): a review of 47 cases. Gynecol Oncol 2016;140:53–7.
27. Foulkes WD, Clarke BA, Hasselblatt M, Majewski J, Albrecht S, McCluggage WG. No small surprise - small cell carcinoma of the ovary, hypercalcaemic type, is a malignant rhabdoid tumour. J Pathol 2014; 233:209–14.
28. Bailey S, Murray MJ, Witkowski L, Hook E, Hasselblatt M, Crawford R, et al. Biallelic somatic SMARCA4 mutations in small cell carcinoma of the ovary, hypercalcemic type (SCCOHT). Pediatr Blood Cancer 2015; 62:728–30.
29. Copeland RA. Evaluation of enzyme inhibitors in drug discovery: a guide for medicinal chemists and pharmacologists. Hoboken, NJ: John Wiley & Sons, Inc.; 2013. p.538.
30. Daigle SR, Olhava EJ, Therkelsen CA, Majer CR, Sneeringer CJ, Song J, et al. Selective killing of mixed lineage leukemia cells by a potent small-molecule DOT1L inhibitor. Cancer Cell 2011;20:53–65.
31. Shalem O, Sanjana NE, Hartenian E, Shi X, Scott DA, Mikkelsen TS, et al. Genome-scale CRISPR-Cas9 knockout screening in human cells. Science 2014;343:84–7.
32. Wang T, Wei JJ, Sabatini DM, Lander ES. Genetic screens in human cells using the CRISPR-Cas9 system. Science 2014;343:80–4.
33. Birmingham A, Selfors LM, Forster T, Wrobel D, Kennedy CJ, Shanks E, et al. Statistical methods for analysis of high-throughput RNA interference screens. Nat Methods 2009;6:569–75.
34. Barretina J, Caponigro G, Stransky N, Venkatesan K, Margolin AA, Kim S, et al. The Cancer Cell Line Encyclopedia enables predictive modelling of anticancer drug sensitivity. Nature 2012;483:603–7.
35. Forbes SA, Bhamra G, Bamford S, Dawson E, Kok C, Clements J, et al. The Catalogue of Somatic Mutations in Cancer (COSMIC). Curr Protoc Hum Genet 2008;Chapter 10:Unit 10 1.
36. Karanian-Philippe M, Velasco V, Longy M, Floquet A, Arnould L, Coindre JM, et al. SMARCA4 (BRG1) loss of expression is a useful marker for the diagnosis of ovarian small cell carcinoma of the hypercalcemic type (ovarian rhabdoid tumor): a comprehensive analysis of 116 rare gynecologic tumors, 9 soft tissue tumors, and 9 melanomas. Am J Surg Pathol 2015;39:1197–205.
37. Le Loarer F, Watson S, Pierron G, de Montpreville VT, Ballet S, Firmin N, et al. SMARCA4 inactivation defines a group of undifferentiated thoracic malignancies transcriptionally related to BAF-deficient sarcomas. Nat Genet 2015;47:1200–5.
38. Domcke S, Sinha R, Levine DA, Sander C, Schultz N. Evaluating cell lines as tumour models by comparison of genomic profiles. Nat Commun 2013; 4:2126.
39. Bitler BG, Aird KM, Garipov A, Li H, Amatangelo M, Kossenkov AV, et al. Synthetic lethality by targeting EZH2 methyltransferase activity in ARID1A-mutated cancers. Nat Med 2015;21:231–8.
40. Kim KH, Kim W, Howard TP, Vazquez F, Tsherniak A, Wu JN, et al. SWI/SNF-mutant cancers depend on catalytic and non-catalytic activity of EZH2. Nat Med 2015;21:1491–6.
41. Grassian AR, Scales TM, Knutson SK, Kuntz KW, McCarthy NJ, Lowe CE, et al. A medium-throughput single cell CRISPR-Cas9 assay to assess gene essentiality. Biol Proced Online 2015;17:15.
42. Konig R, Chiang CY, Tu BP, Yan SF, DeJesus PD, Romero A, et al. A probability-based approach for the analysis of large-scale RNAi screens. Nat Methods 2007;4:847–9.
43. Hoffman GR, Rahal R, Buxton F, Xiang K, McAllister G, Frias E, et al. Functional epigenetics approach identifies BRM/SMARCA2 as a critical synthetic lethal target in BRG1-deficient cancers. Proc Natl Acad Sci U S A 2014;111:3128–33.
44. Wilson BG, Helming KC, Wang X, Kim Y, Vazquez F, Jagani Z, et al. Residual complexes containing SMARCA2 (BRM) underlie the oncogenic drive of SMARCA4 (BRG1) mutation. Mol Cell Biol 2014;34: 1136–44.
45. Glaros S, Cirrincione GM, Muchardt C, Kleer CG, Michael CW, Reisman D. The reversible epigenetic silencing of BRM: implications for clinical targeted therapy. Oncogene 2007;26:7058–66.
46. Italiano A, Keilhack H, Toulmonde M, Coindre JM, Michot JM, Massard C, et al. 302 a phase 1 study of EPZ-6438 (E7438), an enhancer of Zeste-Homolog 2 (EZH2) inhibitor: preliminary activity in INI1-negative tumors. Eur J Cancer 2015;51:S54–S5.